STUDY ON EFFECT OF FUEL INJECTION STRATEGY ON COMBUSTION NOISE AND EXHAUST EMISSION OF DIESEL ENGINE

by

Zhixia HE*, Tiemin XUAN, Zhaochen JIANG, and Yi YAN

School of Energy and Power Engineering, Jiangsu University, Zhenjiang, China

Original scientific paper
DOI: 10.2298/TSCI120603159H

The traditional mechanical fuel supply system has already been no way to satisfy the requirement of more stringent fuel consumption and emission legislation. For the past few years, it has been the hot topic to improve combustion and emission performance of diesel engine through optimizing the fuel injection strategy. All kinds of spray, combustion, and emission models were studied and then a new 3-D spray model coupled with the cavitating flow inside the nozzle was put forward to well consider the primary atomization induced by cavitating flow and turbulence in nozzle holes. The model, combined with combustion and emission models were used for simulating the single-injection combustion of 1015 diesel engine and validated through comparing the results from simulation with those from experiment. With the above verified models, different injection strategies were further investigated to reveal the effect of pilot injection timing, quantity, and main injection timing on combustion noise and exhaust emission of diesel engine.

Key words: *primary atomization model, fuel injection strategy, combustion noise, exhaust emission*

Introduction

The diesel engine has been paid more and more attention because of the better power performance, thermal efficiency, and low emission of CO_2. During the 80s , the well-known advantage of fuel economy made the direct injection (DI) diesel engine increasingly attractive for passenger cars, especially in Europe[1-3]. In the following years the more stringent emission limits and the necessity of reducing noise levels were firstly faced by means of after-treatment technologies, exhaust gas recirculation (EGR) and electronic engine control [4]. Further improvements have been obtained thanks to the common rail fuel injection system, which allows a higher level and a flexible control of the injection pressure and the use of a pilot injection (Pi), which can be controlled both in quantity and in timing [5-7].

It has become an important and urgent task to carry out research of noise reduction for internal combustion engine. The combustion noise is one of the main noise sources for in-cylinder DI diesel engines so that reduction of combustion noise can make a great contribution to the control of the entire noise of diesel engines [8]. For the diesel engine, particles and NO_x emission are two major main pollutants. Using the Pi strategy, the temperature and in-cylinder pressure can be lower so that the NO_x can be greatly reduced. In addition, the fuel and air are mixed more fully and air utilization rate is improved when adoption of the Pi, consequently reduction of soot formation can also be achieved [9, 10].

* Corresponding author; e-mail: zxhe@ujs.edu.cn

In this paper, in order to get the more accurate calculating results, a spray model coupled with the cavitating flow inside the nozzle was put forward. The spray and combustion process in cylinder coupling with a single injection was simulated firstly and a comparison between the numerical data and experimental data was made to validate the numerical models. Then, with the verified models, the combustion and emission in the cylinder with different multiple injection strategies were simulated and analysed to provide theoretical foundation for a better understanding of the effect of different injection strategies on combustion noise and emission.

Table 1. Engine specifications

Engine type	1015 diesel engine
Bore × stroke [mm]	132 × 145
Compression ratio	17
Connection rod length [mm]	262
Engine speed [rpm]	2100
Swirl rate	0.7
Start of injection [°]	350

Table 2. Injection system specifications

Fuel injected [mg per cycle]	180
Number of nozzle holes	8
Spray angle [°]	150
Spray cone angle [°]	12
Nozzle hole diameter [mm]	0.23
Injection pressure [MP]	90

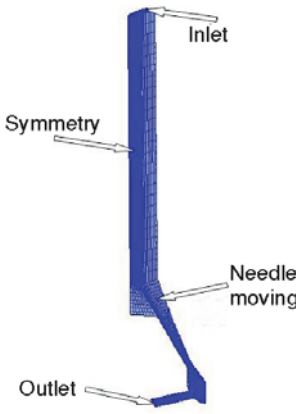

Figure 1. Grid and boundaries of the nozzle

Numerical approach

Calculating meshes

For a 1015 diesel engine, structure parameters and experimental condition parameters are shown in tab.1, the injection system parameters are shown in tab. 2.

The 3-D physical geometry of the vertical eight-hole nozzle was prepared by Pro/E software and a moving mesh generation strategy was applied. The grid has 48.097 cells and 55.168 nodes. For the vertical eight-hole nozzle, the angles between every holes axis and the needle seat axis are same and all the 8 holes are located for proportional spacing along circumference. Thus, only a 22.5° sector zone of mesh needs to be generated for the nozzle. The main boundary conditions are represented with the pressure inlet, corresponding to the rail pressure, the symmetry faces, the moving needle, and the pressure outlet that should reflect the pressure of the injection chamber, as seen in fig.1.

For the spray and combustion simulation, because of the symmetrical location of the injector at the center of the combustion chamber, the computational fluid dynamics (CFD) calculations were performed with the mesh of 45° sector zones [11]. Calculations begin at intake valve closure (218.5°) and end at exhaust valve opening (483°). The final mesh consists of a hexahedral dominated mesh shown in fig. 2.

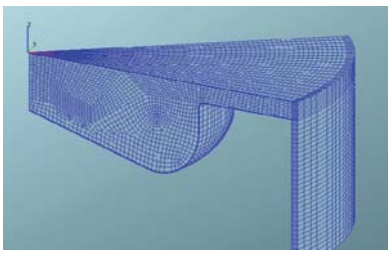

Figure 2. The mesh of combustion chamber

Spray model coupled with nozzle flow

The nozzle flow was modelled with two-fluid model. In two-fluid models, the liquid and vapor phases are treated separately using two sets of con-

servation equations. The model is based on the transport of volume fraction, and a source term representing phase transition that is governed by the difference between local pressure and vapour pressure. Cavitation is assumed to occur due to the presence of bubble nuclei or micro bubbles within the liquid, which can grow or collapse, as described by the vapor fraction transport equation. The growth and collapse of the bubble are taken into account according to the Rayleigh's simplified bubble dynamics equation.

It is assumed that all vapor bubbles in a control volume have the same radius and a homogenous distribution. This assumption allows us to describe the bubble distribution by a single scalar field, the vapor volume fraction α_v. Assuming that only one liquid phase and the corresponding liquid-vapor phase can occupy the control volume where cavitation takes place, eq. (1) gives a relationship between the vapor volume fraction α_v and the average vapor bubble radius R:

$$\alpha_v = \frac{V_v}{V} = \frac{N_{bub}\frac{4}{3}\pi R^3}{V_l + V_v} = \frac{n_0 V_l \frac{4}{3}\pi R^3}{V_l + n_0 V_l \frac{4}{3}\pi R^3} = \frac{n_0 \frac{4}{3}\pi R^3}{1 + n_0 \frac{4}{3}\pi R^3} \tag{1}$$

where V_v is the volume occupied by the vapor, V – the total control volume, V_l – the volume occupied by the liquid, and N_{bub} – the number of vapor bubbles in the control volume.

The vapor volume fraction α_v inside a control volume can change due to convective transport and bubble growth or collapse. The eq. (2) describing the transport of α_v assumes that the vapor density is much smaller than the liquid density and is given by:

$$\frac{\mathrm{d}}{\mathrm{d}t}\int_V \alpha_v \mathrm{d}V + \int_S \alpha_v (v - v_s)\mathrm{d}S = \int_V \frac{n_0}{1 + n_0 \frac{4}{3}\pi R^3}\frac{\mathrm{d}}{\mathrm{d}t}\left(\frac{4}{3}\pi R^3\right)\mathrm{d}V \tag{2}$$

The modeling of cavitation bubble growth rate that appears on the right-hand side of eq. (3), is based on the Lagrangian observation of a cloud of bubbles, and the conventional bubble dynamic (observation of a single bubble in an infinite stagnant liquid). This analysis results in the so-called extended Rayleigh-Plasset equation:

$$R\frac{\mathrm{d}^2 R}{\mathrm{d}t^2} + \frac{3}{2}\left(\frac{\mathrm{d}R}{\mathrm{d}t}\right)^2 = \frac{p_{sat} - p_\infty}{\rho_l} - \frac{2\sigma}{\rho_l R} - 4\frac{\mu_l}{\rho_l R}\frac{\mathrm{d}R}{\mathrm{d}t} \tag{3}$$

where p_{sat} is the saturation pressure corresponding to the temperature at the bubble surface, p_∞ – the pressure of the surrounding liquid, ρ_l and μ_l – are the liquid density and viscosity, respectively, and σ – is the surface tension coefficient.

The cavitation model based on the Rayleigh equation links the rate of change of the bubble radius with the local pressure. In this model both the liquid and vapor density are constant and there is no slip between bubbles and liquid.

A cone injection model was used for the primary break-up of the liquid fuel. The model considering two independent mechanisms, aerodynamic surface wave growth and internal stresses by turbulence, which was originally developed by Huh and Gosman [12] and modified by Bianchi and Pelloni [13], as well as Coricone [14], is used also for the core injection approach. For setting up the liquid core erosion rate it can take into account locally resolved coupling to the nozzle flow as well as estimated average values of nozzle flow turbulence. It is assumed in this model that the turbulent fluctuations in the jet are creating initial perturbations on the jet surface. These grow under the action of aerodynamic pressure forces until they detach

as atomized droplets. The coherent liquid core region at the nozzle exit where primary break-up occurs is calculated from a mass balance at the volume elements of the liquid core delivering the core shape.

Equation (4) shows that the determination of mass loss from this region is set up using the rate approach:

$$\frac{\mathrm{d}R}{\mathrm{d}t} = \frac{L_\mathrm{A}}{\tau_\mathrm{A}} \tag{4}$$

with turbulent length scale L_A calculated from the local values of turbulence kinetic energy and turbulent dissipation by Bianchi and Pelloni [13], as shown in eq. (5):

$$L_\mathrm{A} = C_2 C_\mu \frac{k^{1.5}}{\varepsilon} \tag{5}$$

in the nozzle exit cross-section with $C_\mu = 0.09$. The diameter of the product drops resulting from this model is taken as proportional to the turbulent length scale and equal to the atomization length scale, shown in eq. (6):

$$D_\mathrm{d} = L_\mathrm{A} \tag{6}$$

Thus droplet size depends on the local values of turbulence kinetic energy and turbulent energy dissipation.

The time scale for break-up is calculated from both mechanisms under consideration, which are turbulent and aerodynamic break-up, using weighting coefficients C_1 and C_3. The turbulent time scale is calculated from eq. (7):

$$\tau_\mathrm{T} = C_\mu \frac{k}{\varepsilon} \tag{7}$$

and the aerodynamic time scale is gained from the wave number spectrum of the Kelvin--Helmholtz instability model, which is also basis of the WAVE model. The spectrum of growing waves from aerodynamic theory is evaluated using the double atomization length scale as characteristic value for the wavelength. This yields eq. (8):

$$\tau_\mathrm{W} = L_\mathrm{W} \sqrt{\frac{\rho_\mathrm{g} \rho_l u_\mathrm{rel}^2}{\rho_l + \rho_\mathrm{g}} - \frac{\sigma}{(\rho_l + \rho_\mathrm{g}) L_\mathrm{W}}} \tag{8}$$

The final expression for the overall break-up time is shown in eq. (9):

$$\tau_\mathrm{A} = C_1 \tau_\mathrm{T} + C_3 \tau_\mathrm{W} \tag{9}$$

with constants C_1 and constant C_3 depending on matching with experimental data.

The standard WAVE model was used for modeling of secondary atomization, the k-ε-f approach has been used to take account of turbulent effects.

Combustion and emission model

The ECFM-3Z model was applied for combustion. The ECFM-3Z model was developed by the Groupement Scientifque Moteurs (GSM) consortium specifically for diesel combustion. This is a combustion model based on a flame surface density transport equation and a mixing model that can describe inhomogeneous turbulent premixed and diffusion combustion. The model relies on the ECFM combustion model, previously described on a three areas mixing description. In the ECFM-3Z model, the transport equations are solved for the averaged quanti-

ties of chemical species O_2, N_2, CO_2, CO, H_2, H_2O, O, H, N, OH, and NO. Here, averaged means these quantities are the global quantities for the three mixing zones (that is in the whole cell). Therefore, the term "burnt gases" includes the real burnt gases in the mixed zone (zone F^b in fig. 3) plus a part of the unmixed fuel (zone M^b in fig. 3), and air (zone A^b in fig. 3).

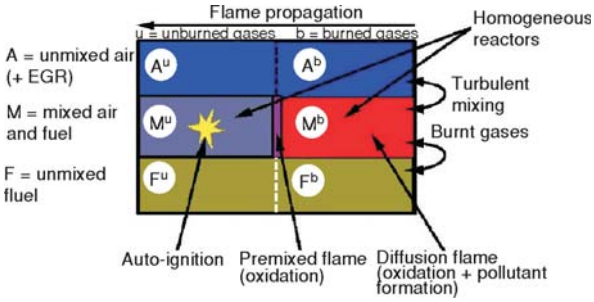

Figure 3. Zones in ECFM-3Z Model

The extended Zeldovich model was used for NO_x formation and Frolov Kinetic model for soot formation and oxidization. All the mathematical equations for these models can seen in reference[15].

Results and discussion

Model validation

Figure 4 shows the comparison between the predicted and measured in-cylinder pressure of single-injection at full road and 2100 rpm speed. The experiment date was got from reference [10]. The results were based on the assumption of uniform temperature of 403 K for the cylinder wall, the temperature of 553 K for the cylinder head and 593 K for the piston top. The in-cylinder pressure curve predicted with the model is reasonably close to experimental data, as can be seen in fig. 4.

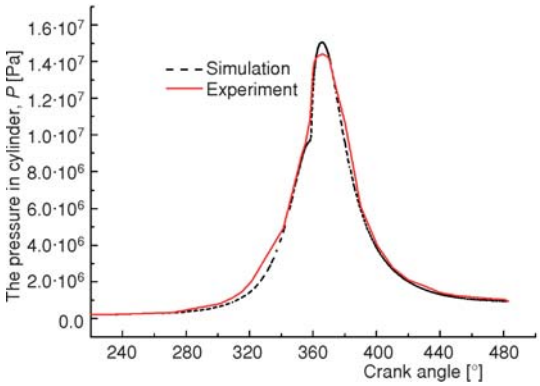

Figure 4. The comparison of pressure between experiment and simulation

Effect of different injection strategies on combustion noise and exhaust emissions

Effect of Pi timing on combustion noise and exhaust emissions

The fuel injection strategies are shown in tab. 3. Combustion noise mainly focuses on high frequency area, which is dominated by rate of in-cylinder pressure rise. The rate of pressure rise, temperature, NO_x and soot emission got from simulation for different injection strategies

Table 3. Injection strategies of different Pi timing main injection*

Injection strategies	Pi quantity	Pi timing [°]	MI timing [°]	Interval [°]
Pi(per 5.335)-M(350)	5%	335-340	350	10
Pi(per 5.325)-M(350)	5%	325-330	350	20
Pi(per 5.315)-M(350)	5%	315-320	350	30
Single	0	–	350	–

* Main injection (MI) timing was fixed at 350°

are given in figs. 5 and 6. Because of the Pi, the temperature and in-cylinder pressure is reduced, which greatly reduced the ignition delay time, so that the highest rate of pressure rise become lower and so does the combustion noise.

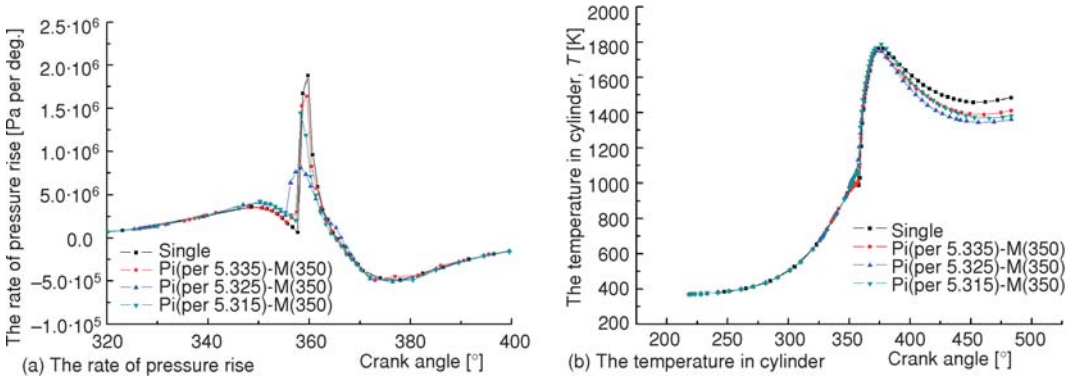

Figure 5. The rate of pressure rise and the temperature in cylinder at different Pi timing

When the interval period between Pi and MI is too large, the influence of PI on main combustion is quite weak because the fuel of Pi is burned quickly and the cylinder has been cold before main combustion, although the fuel of Pi burning fully. As shown in fig. 5(a), comparing with single injection, the rate of pressure rise is changed little when the PI timing is set beginning at 315°. On the other hand, the influence of Pi on main combustion is also little when the interval period is too small, owing to the fuel of Pi could not been burned fully.

It is shown in fig. 5(b) that during most of the time the temperature with Pi is lower than that with single injection. And the NO_x formation is dominated by temperature especially when the temperature is higher than 1800 K. So the NO_x emission was least when the Pi timing is set at 325° corresponding to the lowest in-cylinder temperature, as shown in fig. 6(a). The soot emission with Pi timing at 325° and 315° are both higher than that with single injection at beginning, while after about 422°, the soot emission with Pi are all lower than that with single injection. Especially for a small interval, as Pi timing at 335°, the soot emission is reduced greatly. So the soot emission is reduced because of the reduction of area of high temperature and the low oxygen concentration with pilot injection strategies.

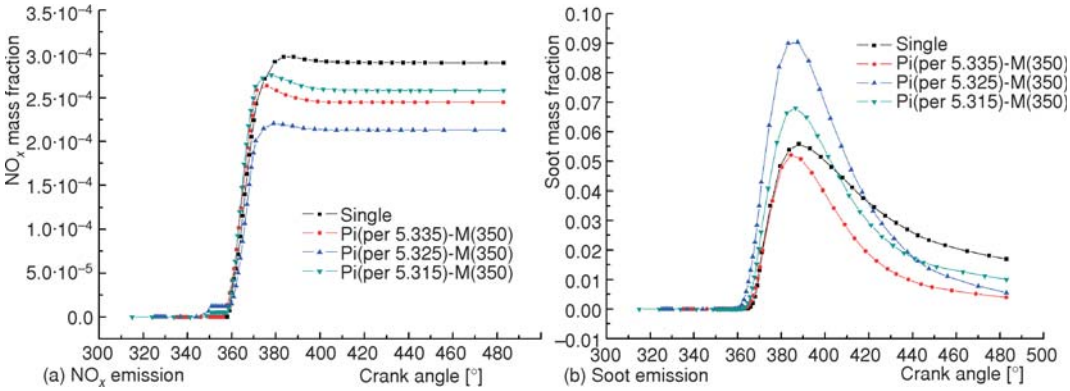

Figure 6. NO_x emission and soot emission at different Pi timing

Effect of Pi quantity on combustion noise and exhaust emissions

In order to analyze the effect of different Pi quantity (2%, 5%, 10% of fuel injected/cycle) on combustion noise and exhaust emissions, the Pi timing was fixed at 325° and the MI timing was fixed at 350°. The injection strategies are shown in tab. 4.

Table 4. Injection strategies of different PI quantity

Injection strategies	Pi quantity	Pi timing [°]	MI timing [°]	Interval [°]
Pi(per 2.325)-M(350)	2%	325-330	350	20
Pi(per 5.325)-M(350)	5%	325-330	350	20
Pi(per 10.325)-M(350)	10%	325-330	350	20
Single	0	–	350	–

Pi timing was fixed at 325° and MI timing was fixed at 350°

As shown in fig. 7(a), when the Pi quantity was 2%, the injection pressure was the same but the amount was so small that injection rate was too low and fuel atomization was poor. In that case, the preheating influence on MI combustion was little, which made the rate of pressure rise a little higher compared with single injection. As a result the combustion noise might be not much different with the single injection. From fig. 7(b) and 7(c), it can be found that the peak of temperature was much higher than that for other injection strategies when the Pi quantity was 10%, which increased the NO_x emission greatly.

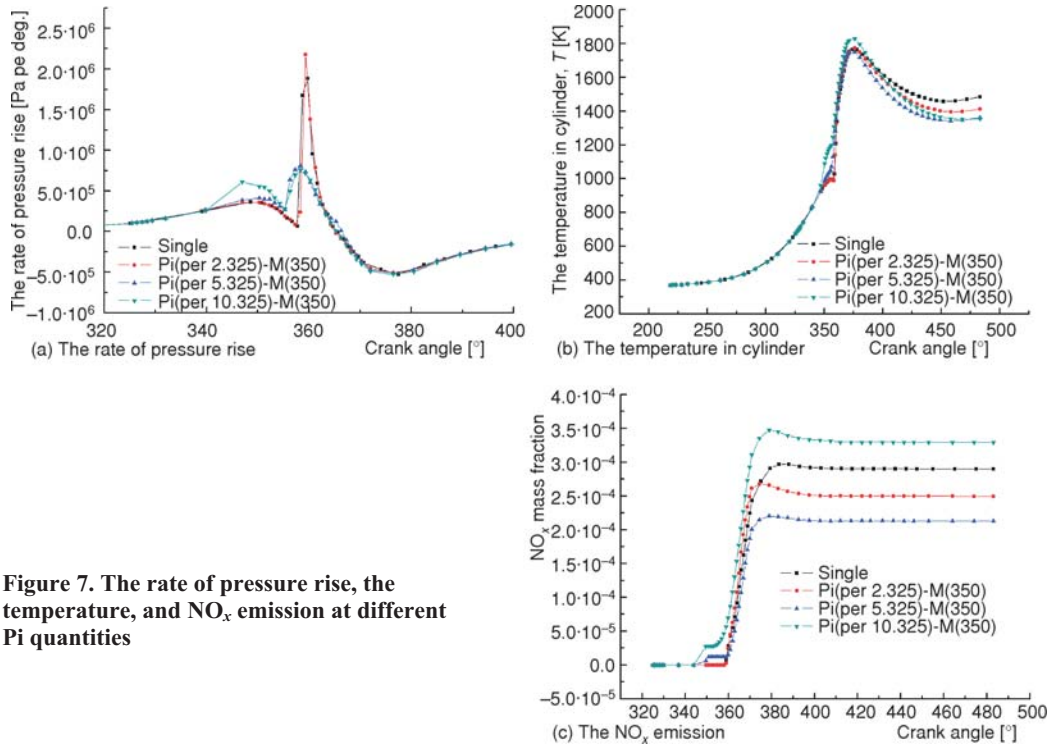

Figure 7. The rate of pressure rise, the temperature, and NO_x emission at different Pi quantities

Effect of MI timing on combustion noise and exhaust emissions

In order to analyze the effect of MI timing on combustion noise and exhaust emissions, different strategies are simulated, as shown in tab. 5.

Table 5. Injection strategies of different MI timing

Injection strategies	Pi quantity	Pi timing [°]	MI timing [°]	Interva [°]
Pi(per 5.325)-M(350)	5%	325-330	350	20
Pi(per 5.325)-M(355)	5%	325-330	355	25
Pi(per 5.325)-M(360)	5%	325-330	360	30
Single	0	–	350	–

Pi timing was fixed at 325° and Pi quantity was fixed at 5%

It can be found from fig. 8(a) that the maximum rate of pressure rise was postponed with the delay of MI advanced angle and the peak reduced obviously when other parameters were fixed. As shown in fig. 8(b), there was no significant difference about the temperature in cylinder with different MI timing, so ignition delay period was almost the same which eventually had little effect on the rate of pressure rise. But the rate of pressure rise was reduced significantly when the MI timing was at 360°, because the piston had gone downside when the MI combustion started. It can be concluded that the combustion noise can be reduced significantly by the appropriate delay of the MI timing. However, the MI timing can not be postponed too much, or the fuel consumption would be increased and the influence of Pi on main combustion would be weakened.

The formation rate of the NO_x increases sharply with the temperature in cylinder as an index function, but it becomes very low when the temperature is lower than 1800 K. It can be seen from fig. 8(b) the average temperature were under 1800 K in all injection strategies, so the difference of the NO_x emission was not dominated by temperature. It can be known from Zeldovich theory of NO_x formation, the generation rate of NO_x is proportional to $P^{1.5}$. The peak of the pressure was reduced obviously with the delay of the MI timing, so the NO_x emission was reduced significantly, as shown in fig. 9(a) and fig. 9(b).

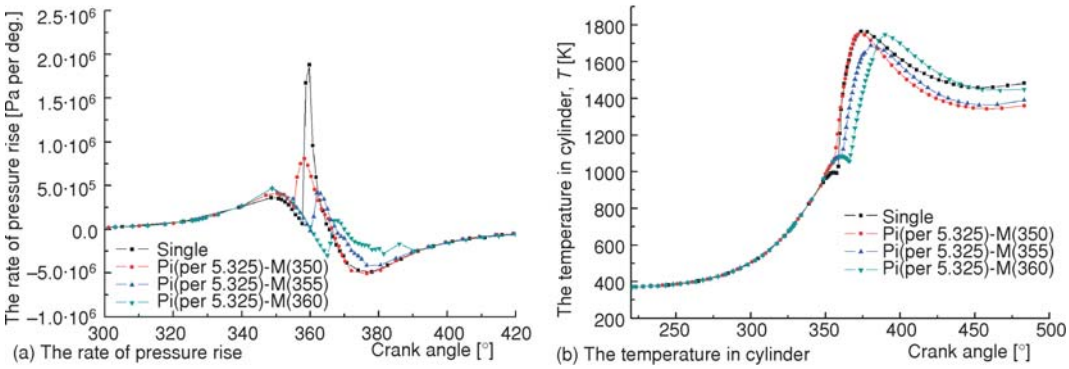

Figure 8. The rate of pressure rise and the temperature in cylinder at different MI timing

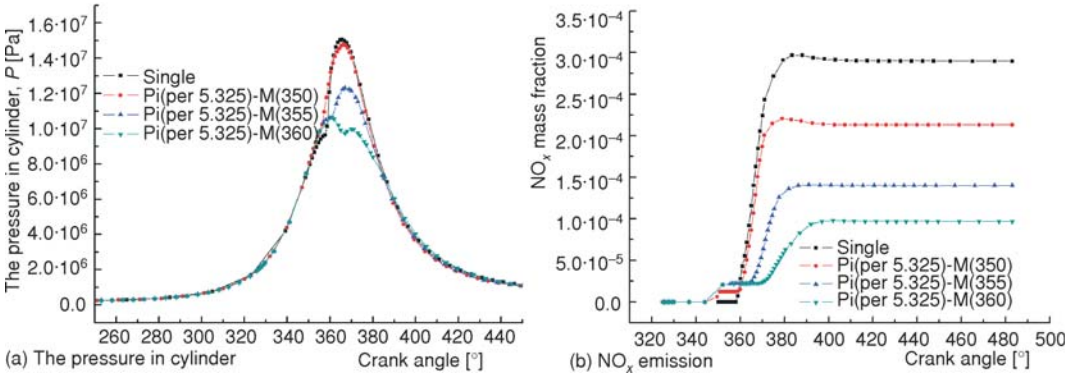

Figure 9. The pressure in cylinder and the NO_x emission at different MI timing

Conclusions

According to the results and analysis, it can be found that the Pi can reduce the in-cylinder combustion noise obviously and improve the emission performance for diesel engines. Bring forward the Pi timing with the MI timing of 350°, the emission of soot is decreased while the combustion noise and the emission of NO_x may have the lowest value at Pi timing of 325°. A small Pi quantity does not have obviously effect on the combustion noise and NO_x emission. When increasing the Pi quantity to 10%, the emission of NO_x is correspondingly increased greatly. When increasing the Pi quantity, the emission of soot had a trend of increasing. When the MI was delayed at Pi timing of 325° and quantity of 5%, the temperature were all under 1800 K and then the emission of NO_x was dominated by pressure in cylinder.

Acknowledgments

This work was supported by the National Natural Science Foundation of China (No. 51176066).

Nomenclature

k – turbulence kinetic energy, [m^2s^{-2}]
L_A – turbulent length scale, [m]
L_W – atomization length scale, [m]
N_{bub} – number of vapor bubbles in the control volume, [–]
R – average vapor bubble radius, [m]
V – total control volume, [m^3]
V_l – volume occupied by the liquid, [m^3]
V_v – volume occupied by the vapor, [m^3]

Greek symbols

α_v – vapor volume fraction, [–]
ε – turbulent energy dissipation, [m^2s^{-3}]
μ_l – liquid viscosity, [ms^{-1}]
ρ_l – liquid density, [kgm^{-3}]
ρ_g – gas density, [kgm^{-3}]
σ – surface tension coefficient, [–]
τ_A – overall break-up time, [s]
τ_T – turbulent time scale, [s]
τ_W – aerodynamic time scale, [s]

Subscripts

bub – vapor bubbles
g – gas
l – liquid
rel – relative
T – time
v – vapor

References

[1] Zhang, X., Study on the Effect of the Injection Strategy on the Combustion and Emission of a Diesel with Electrical Control System, M. Sc. thesis, Dalian University of Technology, Dalian, China, 2010

[2] Morello, L., Martinez, P., FIAT High Speed Direct Injection Diesel Engine for Application on Passenger Cars, SAE paper 890460, 1989
[3] Stock, D., The New Audi-5 Cylinder Turbo Diesel Engine: The First Passenger Car Diesel Engine with Second Generation Direct Injection, SAE paper 900648, 1990
[4] Badami, M., *et al*., Experimental Investigation on Soot and NO_x Formation in a DI Common Rail Diesel Engine with Pilot Injection, SAE paper 2001-01-0657, 2001
[5] Rinolfi, R., Imarisio, R., The Potentials of Third Generation Direct Injection Diesel Engines for Passengers Cars, Engine and Environment International Congress, AVL list Gmbh-Graz, Graz, Austria, 1997
[6] Rinolfi, R., Imarisio, R., The Potentials of a New Common Rail Diesel Fuel Injection System for the Next Generation of DI Diesel Engines, 16th International Wienna Motor Symposium, VDI Verlag, Reihe 12, n. 239, 1995
[7] Ceronetti, G . F., *et al*., Control Strategies and Design Modifications for Exhaust Emission Reduction in Diesel Injection Diesel Engines, FISITA paper 905074, 1990
[8] Zhou, B., Principles of Internal Combustion Engine, Beijing, 2011
[9] Yan, Z., Numerical Analysis about Effect of Multiple Injections on Diesel Engine with the Common Rail Injection System, M. Sc. thesis, Jilin University, Jilin, China, 2008
[10] Zhu, W., Simulation of the Influence of Pilot Injection and Post Injection on the Combustion and Emission of Diesel Engine, M. Sc. thesis, BJTU, Beijing, 2009
[11] ***, AVL_FIRE Engine Simulation Environment (ESE) Tutorial, V2009, 2009.04
[12] Huh, K. Y., Gosman, A.D., A Phenomenological Model of Diesel Spray Atomisation, *Proceedings*, International Conference on Multiphase Flows, 1991, Tsukuba, Japan
[13] Bianchi, G. M., Pelloni, P., Modeling the Diesel Fuel Spray Break-up by Using a Hybrid Model, SAE paper 1999-01-0226, 1999
[14] Corcione, F. E., *et al*., Modeling Atomization and Drop Break-up of High-Pressure Diesel Sprays, *ASME Journal of Engineering for Gas Turbine and Power, 123* (2001), 2, pp. 419-427
[15] ***, AVL_FIRE ICE-Physics-Chemistry, V2010, 2011

Paper submitted: June 3, 2012
Paper revised: August 2, 2012
Paper accepted: September 9, 2012